STUDY OF THE ^{78,86}Kr+^{40,48}Ca REACTIONS AT 10 *A* MeV: COMPARISON WITH THEORETICAL MODELS*

M. Trimarchi[a,b], S. Pirrone[b], G. Politi[b,c], B. Gnoffo[b,c]
J.P. Wieleczko[d], M. La Commara[e,f], E. De Filippo[b]
P. Russotto[g], M. Vigilante[e,f], M. Colonna[g]
Sh.A. Kalandarov[h], F. Amorini[g], L. Auditore[a,b], C. Beck[i]
E. Bonnet[d,j], B. Borderie[k], G. Cardella[b], A. Chbihi[d]
A. D'Onofrio[e,f], J. Frankland[d], E. Geraci[b,c], E. La Guidara[b,l]
G. Lanzalone[g,m], P. Lautesse[n], N. Le Neindre[o]
K. Mazurek[d,p], A. Pagano[b], E.V. Pagano[c,g], M. Papa[b]
E. Piasecki[q,r], L. Quattrocchi[b,c], F. Rizzo[c,g], E. Rosato[e,f]
G. Spadaccini[e,f], A. Trifirò[a,b], G. Verde[b,l]

[a]Dipartimento MIFT — Università degli Studi di Messina, Italy
[b]INFN, Sezione di Catania, Italy
[c]Dipartimento di Fisica e Astronomia, Università di Catania, Italy
[d]Grand Accélérateur National d'Ion Lourds
CEA and CNRS/IN2P3 Caen, France
[e]Dipartimento di Fisica "Ettore Pancini", Università di Napoli Federico II, Italy
[f]INFN, Sezione di Napoli, Italy
[g]INFN Laboratori Nazionali del Sud, Catania, Italy
[h]JINR, Dubna, Russia and Institute of Nuclear Physics, Tashkent, Uzbekistan
[i]Institute Pluridisciplinaire Hubert Curien, Université de Strasbourg, France
[j]SUBATECH, EMN-IN2P3/CNRS — Univeresité de Nantes, France
[k]Institut de Physique Nucléaire, CNRS/IN2P3
Université Paris Sud, Orsay, France
[l]Centro Siciliano Fisica Nucleare e Struttura della Materia, Catania, Italy
[m]Università degli Studi di Enna, "Kore", Italy
[n]IN2P3 — IPN Lyon, France
[o]Laboratoire de Physique Corpusculaire, ENSICAEN, Université de Caen, France
[p]H. Niewodniczński Institute of Nuclear Physics, Polish Academy of Sciences
Kraków, Poland
[q]Heavy Ion Laboratory, University of Warsaw, Warszawa, Poland
[r]National Centre for Nuclear Reasearch, Warszawa, Poland

(Received December 28, 2017)

* Presented at the XXIV Nuclear Physics Workshop "Marie and Pierre Curie", Kazimierz Dolny, Poland, September 20–24, 2017.

In heavy-ion collisions at low energy, the decay mode of the compound nucleus formed in fusion reactions can be strongly influenced by the isospin degree of freedom, strictly connected to the isotopic ratio N/Z of the system. The competition among the disintegration modes of ^{118,134}Ba* produced in ^{78,86}Kr+^{40,48}Ca reactions at 10 A MeV has been studied in the framework of the ISODEC experiment, and experimental data have been compared with the prediction of GEMINI++ and DiNuclear System (DNS) models.

DOI:10.5506/APhysPolBSupp.11.189

1. Introduction

The study of the fusion mechanism in heavy-ion collisions at low energy, leading to the formation of nuclei in extreme conditions of spin and temperature, can provide valuable information on interesting and fundamental aspects of nuclear matter. In particular, the isospin of the Compound Nucleus (CN), strictly connected to the isotopic ratio N/Z of the system, is expected to play an important role in the following emission process, providing crucial information on fundamental quantities, as energy level densities or fission barriers.

In this framework, the ISODEC experiment aimed at studying the competition among the various disintegration modes of ^{118,134}Ba* compound nuclei produced in the reactions ^{78,86}Kr+^{40,48}Ca at 10 A MeV [1–5].

The investigated systems differ for 16 nucleons, that is the maximum difference in neutron numbers achievable for these systems by using stable nuclei: this allows to produce compound nuclei with comparable spin distribution and excitation energies in a large domain of N/Z.

The experiment has been performed at INFN — Laboratori Nazionali del Sud (LNS) in Catania, by means of the CHIMERA 4π multidetector array, allowing us to obtain very accurate measurements of cross sections, multiplicities, angular and kinetic energy distributions of the various reaction products.

Experimental data have been compared with the prediction of GEMINI++ code and DiNuclear System model: results of these comparisons will be presented.

2. Experimental set-up

The experiment has been performed by means of the 4π CHIMERA multidetector array at LNS, characterized by good isotopic resolution, low-energy threshold for LCP and IMFs, high granularity and broad angular acceptance. Due to these features, CHIMERA is very suitable for measurement of the observable of our interest, namely cross sections, multiplicities, angular and kinetic energy distributions of the reaction products.

CHIMERA consists of 1192 detector telescopes, arranged on 9 rings in the forward part, covering a polar angle from 1° to 30°, and 17 rings in spherical configuration, covering the region between 30° and 176°, with a geometrical efficiency up to 94% of the total solid angle [6, 7].

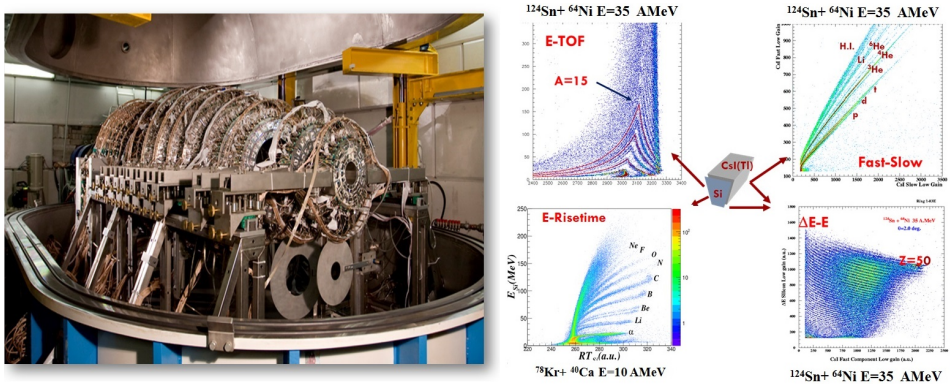

Fig. 1. CHIMERA picture and its particle identification capabilities.

The single detection telescope consists of a planar n-type 300 μm-thick silicon detector, followed by a caesium iodide thallium doped crystal, with thickness ranging from 12 cm at forward angles to 3 cm at backward ones, coupled to a photodiode.

CHIMERA allows us to perform charge and mass identification of detected particles by means of four different techniques [8–11].

For particles stopped in the Si detector, mass identification, velocity and energy measurements can be obtained by means of the E–ToF technique, while the PSD (Pulse Shape Discrimination) method allows us to obtain their charge identification, through rise-time measurement of the energy signals.

For particles punching through the silicon detector, isotopic identification of LCP can be achieved by means of the PSD technique in CsI(Tl), while the traditional ΔE–E technique allows charge identification up to $Z = 50$, and mass identification for particles with $Z < 10$.

3. Experimental results

To investigate the influence of isospin asymmetry on the competition among the different reaction mechanism, let us consider the experimental correlation for the two biggest fragments emitted in complete events, shown in Fig. 2, for the neutron poor (left) and neutron rich (right) systems.

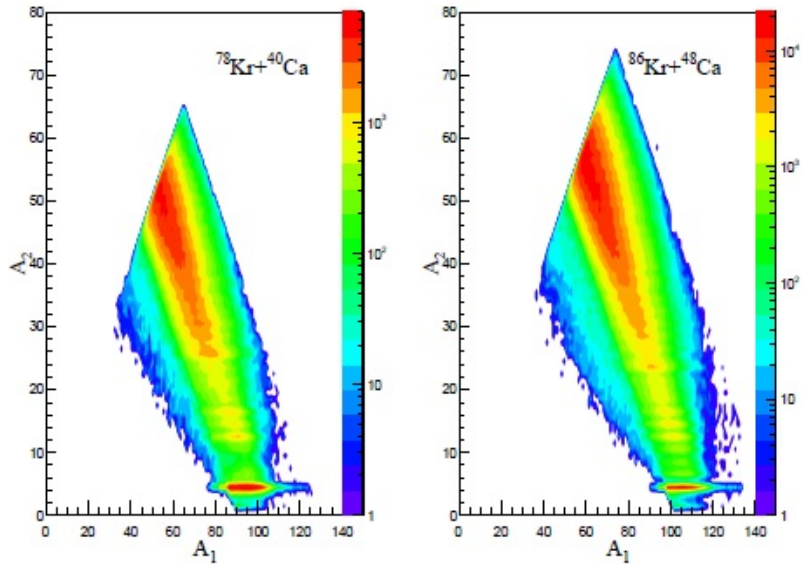

Fig. 2. Correlation plot of the masses of the two biggest fragments detected in complete events for the two reactions.

The region in which $A_1 \gg A_2$, corresponding to the evaporation channel, is more pronounced for the neutron poor system, while the region in which $A_1 \approx A_2$, connected to the symmetric fission mechanism, is more evident for the neutron rich system. These differences evidence the isospin influence on the reaction dynamics.

For what concerns the reaction mechanism, we observed an high degree of relaxation in the fragment production: in the left part of Fig. 3, the average velocities $\langle v_{\mathrm{cm}} \rangle$ of the detected fragments are reported as a function of Z at different detection angles for the neutron poor system.

For any given Z, the $\langle < v_{\mathrm{cm}} \rangle$ is constant with respect to the emission laboratory angle, and its quasi-linear decreasing trend for increasing Z is well-reproduced by the theoretical prediction of the Viola systematic with the corrections by Hinde for the asymmetric fission, providing the most probable energy released in a statistical fission process [12, 13].

This behavior clearly suggests that a high degree of relaxation of the relative kinetic energy has been reached before the occurring of a binary process dominated by the Coulomb interaction between the considered fragment and its complementary partner [14–16].

Moreover, the angular distributions of detected fragments, reported in the right part of Fig. 3, show a general $\frac{1}{\sin\theta}$ behavior, thus confirming that our CN is a long-lived system, having reached a high degree of relaxation.

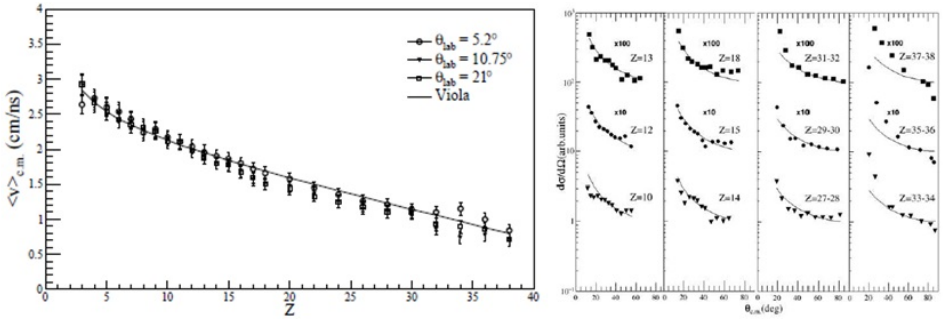

Fig. 3. Left: Velocity of the fragments detected at different angles. Right: Angular distribution of detected fragments for the neutron poor system.

4. Comparison with models

A strong even–odd staggering effect in the charge distributions is observed, due to a preferential production of fragments with an even value of the atomic number. In agreement with other examples in literature [17, 18], this staggering effect is more pronounced for IMFs and for the neutron poor system.

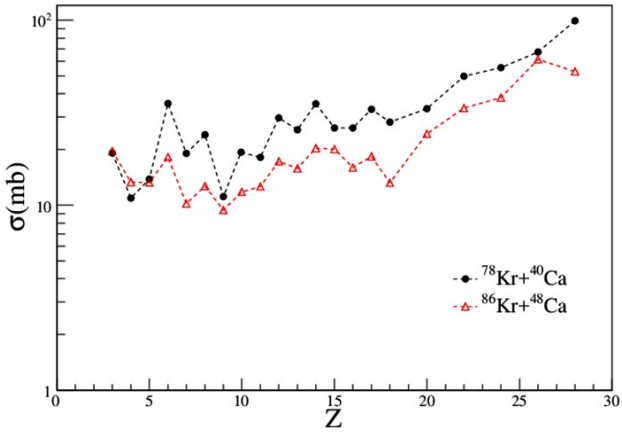

Fig. 4. Experimental charge distributions.

To reproduce the staggering effect and its isospin dependence, the experimental cross sections have been compared with the predictions of the DiNuclear System (DNS) model and of the GEMINI++ code.

These two models have been already used to fit charge distribution for the neutron poor system at lower energy [19, 20].

4.1. Comparison with DNS

According to the DiNuclear System model, the nucleon exchange inside the DNS formed during the reaction path drives the system to the development of a compact configuration, eventually decaying by evaporation, fission, or to the energetically possible dinuclear system configurations which decay by quasi-fission.

The maximum angular momentum $J_{\max}$ compatible with the dinuclear system formation is not a free parameter [21–27], but it is determined by the interaction potential in the entrance channel and by the kinematics: the calculated $J_{\max}$ values are $73\,\hbar$ and $90\,\hbar$ for the neutron-poor and neutron-rich system, respectively.

To calculate the nuclear temperature, which enters the decay formalism, there was used the asymptotical value of the level density parameter $a = 0.114A + 0.162A^{\frac{2}{3}}$ given by Ignatiuk [28], which corresponds to $a \approx \frac{A}{7}$.

Comparison with DNS predictions (combined with HIPSE [29] to evaluate pre-equilibrium emission of light particles) is shown in Fig. 5: the model is unable to reproduce experimental data, though the trend of the charge distribution is qualitatively described [27].

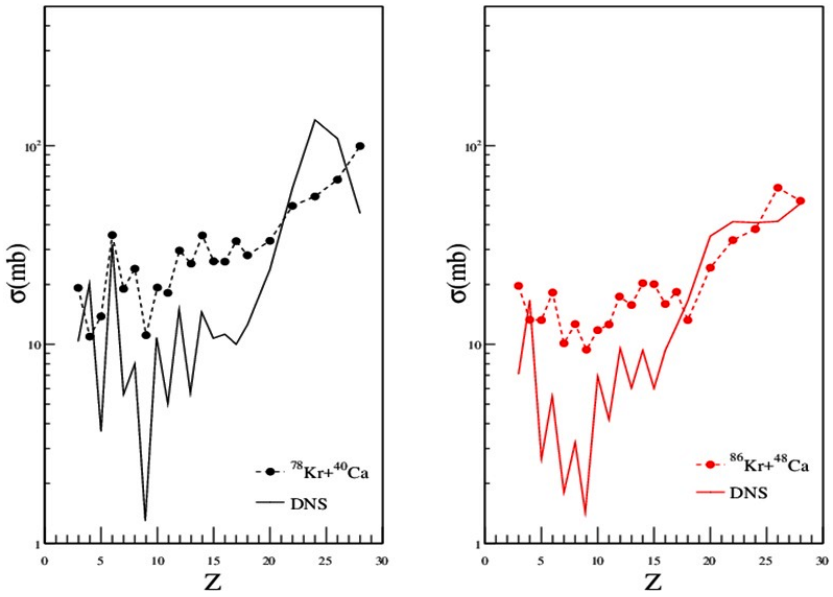

Fig. 5. Comparison with DNS predictions.

The same problem has been observed in the study of the reaction ^{93}Nb+^{27}Al at 11.4 *A* MeV [22], where the DNS model strongly underestimates the production cross sections of the fragments, and a proper description of data would require a very high value of $J_{\max}$.

This suggests that the maximum impact parameter used by the model could be too small: the occurrence of incomplete fusion and quasi fission events at impact parameters larger than those used by the model could then generate the quantitative discrepancy between experimental data and DNS predictions.

This point deserves further investigations: the comparison with the predictions of the stochastic microscopic transport models [30, 31] may shed light on the interplay between the possible reaction mechanisms as a function of the impact parameter.

It has to be noticed that the staggering effect is reproduced, but in the calculations the amplitude is larger: this discrepancy may be removed by considering the excitation energy dependence of the pairing energy, and by fitting the level density parameter to the experimental results.

4.2. Comparison with GEMINI++

The statistical model based on GEMINI++ code [32–38] not only allows light-particle evaporation and symmetric fission, but all possible binary decays of a compound nucleus.

The maximum angular momentum $J_{\max}$ is an input parameter of the code, and can be calculated by means of the Bass Model [39, 40] or constrained from systematics or from experimental data [36].

To establish a connection with the results of the DNS model, we have taken the same $J_{\max}$ values previously used, namely $73\,\hbar$ and $90\,\hbar$, for neutron-poor and neutron-rich system, respectively, and a constant value $\frac{A}{7}$ for the level density parameter.

In Fig. 6, the experimental charge distribution of the reaction products is compared with the predictions of GEMINI++: the obtained behavior is quite different from that predicted by DNS, especially for $Z > 15$.

These two models, although using the same values for $J_{\max}$ and a, substantially differ in describing reaction dynamics. DNS tends to favor a fission-like dynamics, whereas GEMINI++ only assumes CN formation, leading to a lower fragment yield.

Moreover, GEMINI++ calculations do not take into account pre-equilibrium effects that can increase the cross section associated with heavy fragments, and can be significant at 10 *A* MeV for mass-asymmetric reactions such as those in study [41].

One of the causes of the discrepancies observed in the GEMNI++ calculations, for fragments with $Z < 8$, can be related to the transmission coefficients, *i.e.* the most crucial parameters in the Hauser–Feschbach formalism: they are relatively well-known for not too exotic sources, but in such cases as the ^{86}Kr+^{48}Ca reaction, during which the very neutron-rich emitters can be populated, nothing is established.

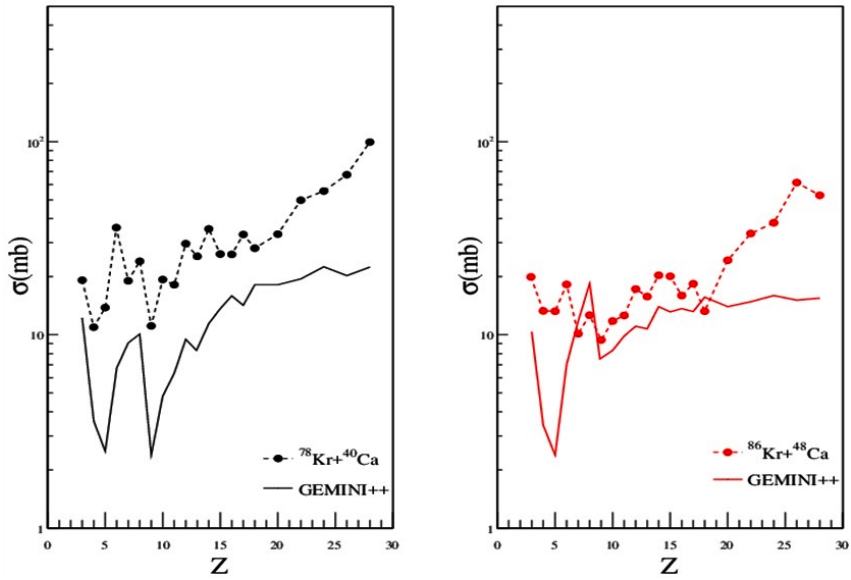

Fig. 6. Comparison with GEMINI++ predictions.

Furthermore, as illustrated in [42], GEMINI++ (as DNS do) fails to reproduce the experimental cross section of the reaction ^{93}Nb+^{27}Al at 11.4 A MeV, and a proper description of data would require a very high value of $J_{\max}$, exactly as it happens for the systems in study.

5. Conclusions

For the ^{78,86}Kr+^{40,48}Ca reactions at 10 A MeV, both DNS and GEMINI++ codes underestimate the fragment production cross section, while they give a good reproduction of experimental cross sections for the ^{78,82}Kr+^{40}Ca reactions at 5.5 A MeV.

For the higher energy reactions, larger impact parameters with respect to those considered in the calculations seem to contribute to the considered reaction mechanism: a proper description of data would require a very high angular momentum, as for the ^{93}Nb+^{27}Al reaction at 11.4 A MeV.

This similarity could suggest that a very exotic system is created during the reaction studied in the ISODEC experiment, whose features cannot be well-reproduced by the used models.

A further comparison with stochastic microscopic transport model calculation will be performed that probably would be able to shed light on competition between different decay modes.

REFERENCES

[1] G. Politi *et al.*, *EPJ Web Conf.* **21**, 02003 (2012).

[2] G. Politi *et al.*, *JPS Conf. Proc.* **6**, 030082 (2015).

[3] S. Pirrone *et al.*, *AIP Conf. Proc.* **1524**, 7 (2013).

[4] S. Pirrone *et al.*, *J. Phys.: Conf. Ser.* **515**, 012018 (2014).

[5] B. Gnoffo, *Il Nuovo Cim. C* **39**, 275 (2016).

[6] A. Pagano *et al.*, *Nucl. Phys. A* **681**, 331 (2001).

[7] A. Pagano *et al.*, *Nucl. Phys. A* **734**, 504 (2004).

[8] A. Pagano *et al.*, Proc. of the XLII Int. Winter Meeting on Nuclear Physics, Bormio, Italy, 2004, ed. I. Iori, p. 359.

[9] G. Politi *et al.*, *IEEE NSS Conf. Record* **N28**, 1140 (2006).

[10] M. Alderighi *et al.*, *IEEE Trans. Nucl. Sci.* **52**, 1624 (2006).

[11] R. Bassini *et al.*, *IEEE NSS Conf. Record* **N14**, 173 (2006).

[12] V.E. Viola *et al.*, *Phys. Rev. C* **31**, 1550 (1985).

[13] D. Hinde *et al.*, *Nucl. Phys. A* **472**, 318 (1987).

[14] R.J. Charity *et al.*, *Nucl. Phys. A* **476**, 516 (1988).

[15] K.X. Jing *et al.*, *Nucl. Phys. A* **645**, 203 (1999).

[16] F. Auger *et al.*, *Phys. Rev. C* **35**, 190 (1987).

[17] I. Lombardo *et al.*, *Phys. Rev. C* **84**, 024613 (2011).

[18] G. Casini *et al.*, *Phys. Rev. C* **86**, 011602 (2012).

[19] G. Ademard *et al.*, *Phys. Rev. C* **83**, 054619 (2011).

[20] G. Ademard *et al.*, *EPJ Web Conf.* **17**, 10005 (2011).

[21] Sh.A. Kalandarov *et al.*, *Phys. Rev. C* **82**, 044603 (2010).

[22] Sh.A. Kalandarov *et al.*, *Phys. Rev. C* **83**, 054611 (2011).

[23] Sh.A. Kalandarov *et al.*, *Phys. Rev. C* **84**, 054607 (2011).

[24] Sh.A. Kalandarov *et al.*, *Phys. Rev. C* **84**, 064601 (2011).

[25] Sh.A. Kalandarov *et al.*, *Phys. Part. Nucl.* **43**, 825 (2012).

[26] Sh.A. Kalandarov *et al.*, *Phys. Rev. C* **90**, 024609 (2014).

[27] Sh.A. Kalandarov *et al.*, *Phys. Rev. C* **93**, 024613 (2016).

[28] A.V. Ignatiuk, *Statistical Properties of Excited Atomic Nuclei*, Energoizdat, Moscow, 1983.

[29] D. Lacroix, A. Van Lauwe, D. Durand, *Phys. Rev. C* **69**, 054604 (2004).

[30] L. Shvedov, M. Colonna, M. Di Toro, *Phys. Rev. C* **81**, 054605 (2010).

[31] C. Rizzo, M. Colonna, V. Baran, *Phys. Rev. C* **90**, 054618 (2014).

[32] H. Hauser, H. Feshbach, *Phys. Rev.* **87**, 366 (1952).

[33] L.G. Moretto, *Nucl. Phys. A* **247**, 211 (1975).

[34] A.J. Sierk, *Phys. Rev. Lett.* **55**, 582 (1985).

[35] N. Carjan, J.M. Alexander, *Phys. Rev. C* **38**, 1692 (1988).

[36] D. Mancusi, R.J. Charity, J. Cugnon, *Phys. Rev. C* **82**, 044610 (2010).
[37] N. Bohr, J.A. Wheeler, *Phys. Rev.* **56**, 426 (1939).
[38] A.Y. Rusanov *et al.*, *Phys. At. Nucl.* **60**, 683 (1997).
[39] R. Bass, *Phys. Lett. B* **47**, 139 (1973).
[40] R. Bass, *Nucl. Phys. A* **231**, 45 (1974).
[41] H. Morgenstern *et al.*, *Phys. Rev. Lett.* **52**, 1104 (1984).
[42] R.J. Charity *et al.*, *Nucl. Phys. A* **483**, 371 (1988).